

# Modeling The Growth Of A Fission Yeast Cell Using The Self-Similarity Growth Principle - A Simplified Approach

Najib A. Kasti  
Beirut Arab University  
Beirut, Lebanon  
e-mail: najib01@idm.net.lb

**Abstract**—Simulating the growth of a cell is vital to the successful modeling of the cell reproduction cycle. Availability of representative simulation parameters is a prerequisite to building these models. Fission yeast cells are good candidates to test these growth models since they are easy to manipulate and their growth data are readily available.

One of the models used to simulate the growth of fission yeast cells assumed growth to be associated with the plasmolysed state of the cell and the elastic deformation being driven by the large turgor pressure. The strain rate of growth was assumed to depend on the elastic strain and a growth function. This growth function is related to the distribution of growth material deposited along the meridian. Fission yeast cells grow from the old and new ends with the width of the cell remaining constant. Also, the growth from the old end maintains an almost constant curvature. These observations were used in this paper to justify the application of the concept of self-similarity of growth to the old end.

In the calculations both a constant as well as variable strain distributions were assumed along the meridian. In addition, the simulation time step was varied to determine its effect on the growth function.

**Keywords**—fission yeast cell; self-similarity growth; turgor pressure; plasmolysed configuration; mechanics; exocytic factors

## I. INTRODUCTION

Modeling systems in mechanics may be attempted at several levels such as: quantum, molecular and micro-scale [1-4]. Modeling the growth of cells could be complex since it encompasses the consideration of several processes and variables. Yeast cells have the advantage of being relatively easy to manipulate, observe and measure. However, an important factor that distinguishes fission yeast cells from most other cells is their high value of turgor pressure which may exceed 1MPa. This pressure leads to large elastic deformations in plasmolysed cells with strains in the order of 20%. When modeling the growth of fission yeast cells the above two factors need to be taken into account [5,6].

The cell cycle of a yeast cell starts after cell division, with growth initially from the Old End (OE) followed by the New End (NE), i.e., location of septation. Growth continues until the cell length almost doubles, as shown in Fig. 1.

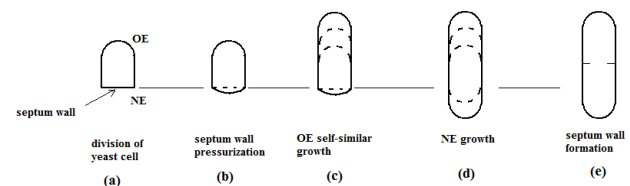


Fig. 1. Fission yeast cell growth cycle

In modeling the growth of the cell, mechanics was determined to be one of two fields instrumental in simulating the cell growth [5-11]. The second field, molecular biology, and specifically the distribution patterns of exocytic factors, influenced the growth shapes [5]. Other publications assumed the distribution of Cdc42 as the influential factor [6].

During the growth of fission yeast, it was observed that the taper of the OE was sharper than a hemispherical taper [5]. On the other hand, the NE starts as being flat, then becomes hemispherical and finally tends to the OE shape.

The curvature of the OE was found to remain almost constant with time and the expansion of the cell wall was limited to the tips of the cell [5]. The growth velocity of fission yeast cells is approximately of the order of  $2\mu\text{m/hr}$  at the OE [7].

In modeling the growth of fission yeast cells three configurations were used [5,6] :

- The plasmolysed configuration.
- The growth configuration due to material deposition.
- The elastically deformed cell configuration driven by the turgor pressure.

The strain rate of growth was assumed to depend on the elastic strain and a growth function that represents the distribution of material deposited along the meridian [5,6].

Since the shape of the OE as well as the diameter of the cell were constant with time, the concept of self-similarity of growth was used in this paper. This concept was combined with mechanics to determine

the distribution of the growth function along the meridian. The strains in the cell are assumed to have two components, elastic and viscous. The elastic strain is large due to the high value of turgor pressure. However, due to small time integration steps, the growth from the viscous strain is assumed to be small between time increments.

Only the OE section was modeled in this work. For ease of presentation of the numerical integration scheme, the initial plasmolysed shape was assumed to be hemispherical. The material deposition during a time step is assumed to change the OE based on the self-similarity concept, i.e., from a hemisphere into another identical hemisphere plus a vertical section equal to the growth of the tip of the cell.

Two strain distributions along the tip of the cell were used. The first one treats the cell tip as basically an isolated half sphere, thus neglecting the effect of the vertical cell wall. In this case the meridional and circumferential strains are equal and constant. The second distribution uses the strains obtained from the finite element modeling of the upper symmetrical half of the cell. This results in a higher distribution of the circumferential strain near the vertical wall. The results of both cases are presented.

To determine the effect of changing the integration time step on the growth function, the results of the growth function from two different time steps are also presented.

## II. LINE MODEL TO DETERMINE THE GROWTH FUNCTION

The following system of equations govern the modeling of fission yeast growth:

The meridian and circumferential elastic strains ( $\epsilon_s^e, \epsilon_\theta^e$ ) depend on the turgor pressure  $P$  and the elastic material properties with  $\epsilon^e = \epsilon^e(P, E, \nu)$  where  $E$  is the elastic modulus and  $\nu$  the Poisson's ratio.

The growth strain rates of wall material ( $d\epsilon_s^g/dt, d\epsilon_\theta^g/dt$ ) will cause the stress-free wall of the plasmolysed cell to grow. The growth strain rates are computed using:

$$d(\epsilon_s^g)/dt = \alpha \cdot \phi(s) \cdot \epsilon_s^e \quad \text{and} \quad d(\epsilon_\theta^g)/dt = \alpha \cdot \phi(s) \cdot \epsilon_\theta^e \quad (1)$$

where  $\alpha$  is a growth factor and  $\phi(s)$  is the growth function that depends on the meridional distance,  $s$ , measured from the tip of the OE. The value of  $\phi(s)|_{s=0}$  is 1.

In modeling the growth of fission yeast three configurations were used, as shown in Fig. 2 [5,6]:

- The plasmolysed configuration "0".
- The elastically deformed cell configuration by turgor pressure "1".
- The configuration where material deposition and growth occur within the cell under turgor pressure "2".

The plasmolysed configuration "0" when subjected to turgor pressure expands to configuration "1" with large elastic deformations. Material deposition, which softens the cell wall, when coupled with the turgor pressure lead to configuration "2".

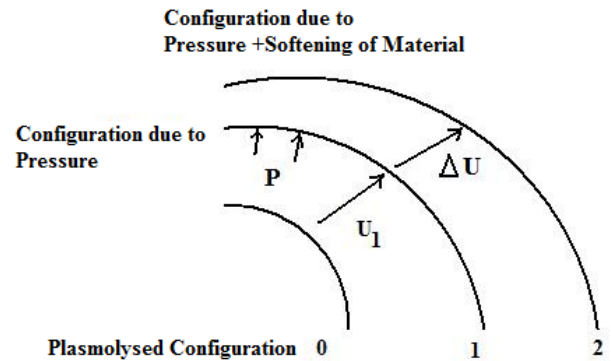


Fig. 2 The three configurations of growth of a fission yeast cell

Two cases were considered for the strain distribution along the OE of the cell.

A. The first one treats the cell tip as basically an isolated half sphere, thus neglecting the effects of the vertical cell wall. In this case the meridional and circumferential strains are equal and constant.

B. The second distribution uses the strains obtained from modeling the upper half of a symmetrical cell. This results in a higher distribution of the circumferential strain near the vertical wall.

These two cases are presented below.

### A. Meridional and Circumferential Strains equal and constant

The strains resulting from the turgor pressure as well as the concept of self-similarity allow us to determine the distribution of the growth function  $\phi(s)$  as follows:

Using small growth strains and a forward-Euler integration scheme, the meridional and circumferential growth strains are expressed as shown below for a time increment  $\Delta t$  from time  $t_m$  to time  $t_{m+1}$ :

$$\begin{aligned} (\epsilon_s^g)_{m+1} &= (\epsilon_s^g)_m + \alpha \cdot \phi(s) \cdot \epsilon_s^e \cdot \Delta t \quad \text{and} \\ (\epsilon_\theta^g)_{m+1} &= (\epsilon_\theta^g)_m + \alpha \cdot \phi(s) \cdot \epsilon_\theta^e \cdot \Delta t \end{aligned} \quad (2)$$

The initial hemispherical shape of radius  $R_0$  is divided into  $n$  elements with  $n+1$  nodes,  $A_1$  to  $A_{n+1}$ . The self-similarity growth principle assumes the initial hemispherical shape ( $A_1, A_{n+1}$ ) with radius  $R_0$  is deformed into a self-similar hemispherical shape ( $a_1, a_n$ ) with the wall of the cell growing vertically by ( $a_n, a_{n+1}$ ), as shown in Fig. 3.

The deformation leading to the self-similar configuration is assumed to be solely due to the viscous growth strains. After this configuration is

reached, the new vertical part ( $a_n, a_{n+1}$ ) solidifies and the process is repeated with conditions similar to the ones at the initial configuration.

By enforcing the location of nodes  $a_1$  to  $a_n$  to be on the self-similar configuration, the growth function  $\phi$  and growth parameter  $\alpha$  are determined as follows:

Let  $L_o$  be the length of segment  $A_i A_{i-1}$  where  $L_o = 2 * R_o * \sin(\pi/(4 * n))$ .

Since the radius of the cell is almost constant during growth, node  $A_{n+1}$  is assumed fixed.

1) Location of node  $a_n$

When node  $A_n$  with coordinates  $(R_{A_n}, Z_{A_n})$  moves to  $a_n(R_o, \text{height})$ , the radial motion  $u_r$  of  $A_n$  and the extension of  $(A_n, A_{n+1})$  are given by:

$$u_r = R_{A_n} * \epsilon_{\theta}^e = R_{A_n} * \alpha * \phi(s_{A_n}) * \epsilon_{\theta}^e * \Delta t = R_o - R_{A_n} \Rightarrow \alpha * \phi(s_{A_n}) = (R_o / R_{A_n} - 1) / (\epsilon_{\theta}^e * \Delta t) \quad (3)$$

and,

$$a_{n+1} a_n = A_{n+1} A_n * (1 + [\epsilon_{s,av}^g]) = A_{n+1} A_n * (1 + \alpha * (1/2) * (\phi(s_{A_{n+1}}) + \phi(s_{A_n})) * \epsilon_s^e * \Delta t) = v * \Delta t \quad (4)$$

where  $v$  is the velocity of tip growth.

Replacing (3) into (4) and noting that  $\phi(s_{A_{n+1}}) = 0$ , we get

$$A_n A_{n+1} * (1 + (1/2) * (R_o / R_{A_n} - 1) * (\epsilon_s^e / (\epsilon_{\theta}^e))) = v * \Delta t \quad \text{or} \quad \Delta t = (A_n A_{n+1} / v) * (1 + (1/2) * (R_o / R_{A_n} - 1) * (\epsilon_s^e / (\epsilon_{\theta}^e))) \quad (5)$$

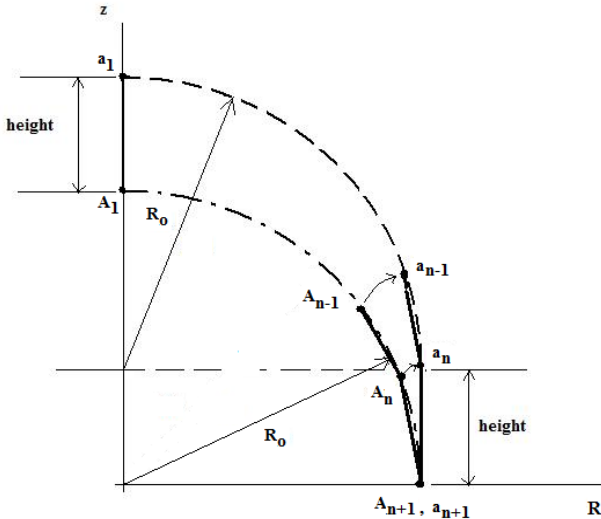


Fig. 3 Self-Similarity of Growth

2) Location of node  $a_i, i < n$

For nodes  $a_{n-1}$  to  $a_1$  the process is continued as follows:

When node  $A_{n-1}$  moves to  $a_{n-1}$  the new radial location of  $a_{n-1}$  and the extension of  $A_{n-1} A_n$  are given by:

$$R_{a_{n-1}} = R_{A_{n-1}} * (1 + \alpha * \phi(s_{A_{n-1}}) * \epsilon_{\theta}^e * \Delta t) \quad (6)$$

and,

$$a_{n-1} a_n = A_{n-1} A_n * (1 + \alpha * (1/2) * (\phi(s_{A_{n-1}}) + \phi(s_{A_n})) * \epsilon_s^e * \Delta t) \quad (7)$$

Node  $a_{n-1}$  should lie on a circle of radius  $R_o$  with  $a_{n-1} a_n$  satisfying

$$(R_{a_{n-1}} - R_{a_n})^2 + (Z_{a_{n-1}} - Z_{a_n})^2 = (a_{n-1} a_n)^2 \quad (8)$$

Substituting (6) and (7) into (8) leads to the nonlinear equation F:

$$F = (R_{A_{n-1}} (1 + \alpha * \phi(s_{A_{n-1}}) * \epsilon_{\theta}^e * \Delta t) - R_{a_n})^2 + (Z_{a_{n-1}} - Z_{a_n})^2 - (A_n A_{n-1} * (1 + \alpha * (1/2) * (\phi(s_{A_n}) + \phi(s_{A_{n-1}})) * \epsilon_s^e * \Delta t))^2 = 0 \quad (9)$$

To determine  $\alpha * \phi(s_{A_{n-1}})$  given  $\alpha * \phi(s_{A_n})$  we need to solve the nonlinear equation using a Newton iteration scheme based on linearizing F about  $\alpha * \phi(s_{A_{n-1}})|_o$ , such as:

$$F_{\text{linear}} = F|_o + (\alpha * \phi - \alpha * \phi|_o) * (dF/d\alpha\phi)|_o = 0 \quad (10)$$

Thus,

$$\alpha * \phi = \alpha * \phi|_o - (F|_o) / (dF/d\alpha\phi)|_o \quad (11)$$

with  $dR_{a_{n-1}}/d[\alpha * \phi(s_{A_{n-1}})]$  and  $dZ_{a_{n-1}}/d[\alpha * \phi(s_{A_{n-1}})]$  determined from (6) and the fact that node  $a_{n-1}$  lies on a circle of radius  $R_o$  and center  $(0, v * \Delta t)$ , respectively.

B. Variable Meridional and Circumferential strains

In case the upper half of the cell of Fig. 1(e) is modeled using the finite element method with symmetric boundary conditions, the circumferential strain would differ from the meridional strain in the hemispherical part close to the vertical cell wall. The above algorithm was modified to take into account the variations of the meridional and circumferential strains with the meridional distance.

III. SIMULATION RESULTS

Once the distribution of  $\alpha * \phi(s_{A_i})$  is determined along the meridian, the value of the growth parameter  $\alpha$  could be determined from  $\alpha = \alpha * \phi(s_{A_i})|_{i=1}$  since  $\phi(s_{A_1}) = 1$ .

Solving the above system for  $R_o = 2.42 \mu\text{m}$ ,  $n = 100$ , velocity of growth of the OE  $v = 2 \mu\text{m/hr}$  and  $\epsilon_s^e = \epsilon_{\theta}^e = 0.1$  leads to the value of  $\alpha = 0.13895$ ,  $\Delta t = 1.14$  minutes and the distribution  $\phi(s_{A_i})$  as shown in Fig. 4.

In the above simulation only one segment  $(A_{100}, A_{101})$  became vertical with a height equal to the tip growth.

The tip growth of the OE is  $0.038 \mu\text{m}$  in this case.

To determine the effect of using a different time step on the self-similarity of growth, the hemisphere was modeled using 201 nodes with only the first segment  $(A_{200}, A_{201})$  becoming vertical. This leads to a value of  $\alpha = 0.13839$  and  $\Delta t = 0.57$  minutes. The tip growth of the OE is  $0.019 \mu\text{m}$  in this case. Thus, half the time for half the growth.

The distributions of the growth functions for  $n=100$  and  $n=200$  are plotted in Fig.4. The relative error between the two growth functions,  $[(\alpha\phi_{200(i)}-\alpha\phi_{100(i)})/\alpha\phi_{100}]*100$  is less than 0.4%. From the above results, with a time step that leads to small growth strains between self-similar configurations, the value of the time step used does not have a considerable effect on the growth function. To estimate the change in the  $\alpha\phi$  function due to variable meridional and circumferential elastic strains along the meridians, a plot of the growth function for a constant and variable meridional (ees) and circumferential (eet) elastic strains is shown in Fig. 5. This corresponds to nodes along the middle of the cell thickness. Twenty elements were used in the analysis with  $Ro=2.1\mu\text{m}$ . The two curves are very close with an error relative to  $\alpha\phi(1)$  of less than 3%.

#### IV. CONCLUSIONS

Several models have been devised to simulate the growth of fission yeast cells. One such model assumed growth is associated with the plasmolysed state of the cell and the large turgor pressure as being the driver of the elastic deformation. The strain rate of growth was assumed to depend on the elastic strain and a growth function  $\phi$ .

Using the above as a basis for the growth model, the paper accomplished/showed the following:

1. Since the shape of the OE and the thickness of the cell were observed to be almost constant with time, the principle of self-similarity of growth was assumed to apply to the OE.
2. The growth factor  $\alpha$  and growth function  $\phi(s)$  were determined using a line model of the cell wall.
3. The difference between the growth functions using a hemispherical model and a half cell model were small.
4. When the growth strains between self-similar configurations are small, the value of the time step used to simulate the growth has little effect on the distribution of the growth function.

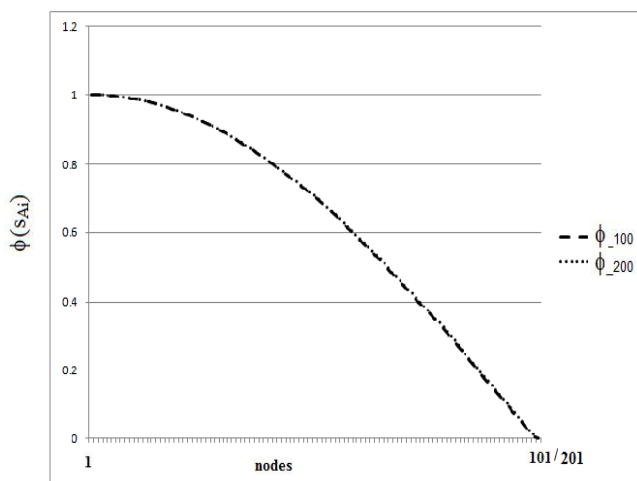


Fig 4. Distribution of growth function  $\phi(S_{Ai})$  due to  $n=100$  and  $200$

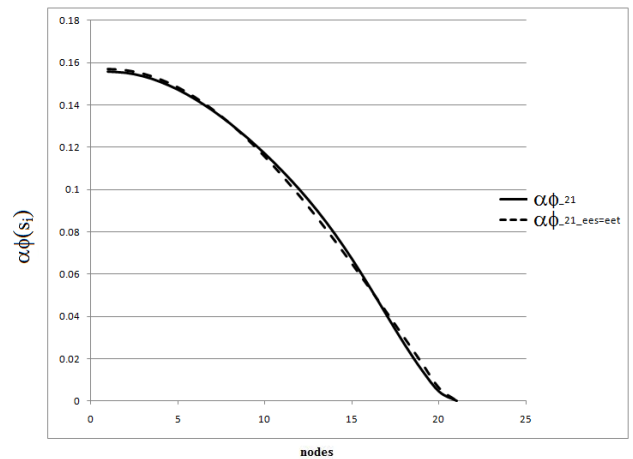


Fig. 5 Distribution of the growth function  $\alpha\phi(S_{Ai})$  due to  $n=20$  and constant/variable elastic strains for the middle nodes

#### REFERENCES

- [1] N. Kasti, "Zigzag carbon nanotube: molecular/structural mechanics and the finite element method," International Journal of Solids and Structures (Elsevier), vol. 44, Issue 21, pp. 6914-6929, 2007.
- [2] N. Kasti, "Zigzag carbon nanotubes under simple torsion – structural mechanics formulation," Advanced Materials Research, v. 452-453, pp. 1139-1143, 2012.
- [3] N. Kasti, "Carbon nanotubes under simple tension and torsion – molecular/structural mechanics and the finite element method," Physical and Chemical Properties of Carbon Nanotubes", Dr. Satoru Suzuki (Ed.), ISBN: 978-953- 51-1002-6, InTech, 2013.
- [4] N. Kasti, "Solution procedure for a class of band structures – application of the finite element method to Schrödinger's equation," Journal of Basic and Applied Physics, v. 3, Issue. 2, pp. 129-138, 2014.
- [5] J. Abenza et al., "Wall mechanics and exocytosis define the shape of growth domains in fission yeast," Nature Communications, 6:8400, doi: 10.1038/ncomms9400, 2015.
- [6] T. Drake and D. Vavylonis, "Model of fission yeast cell shape driven by membrane-bound growth factors and the cytoskeleton," PLOS Computational Biology, Vol. 9, Issue 10, 2013.
- [7] J. Mitchison and P. Nurse "Growth in cell length in the fission yeast Schizosaccharomyces Pombe," J. Cell Sci., 75, pp. 357-376, 1985.
- [8] R. Bernal, E. Rojas and J. Dumais, "The mechanics of tip growth morphogenesis: what we have learned from rubber balloons," Journal of Mechanics of Materials and Structures, Vol. 2, No. 6, 2007.
- [9] E. Atilgan, V. Magidson, A. Khodjakov and F. Chang, "Morphogenesis of the fission yeast cell through cell wall expansion," Current Biology, 25(16), pp. 2150-2157, 2015.
- [10] O. Campas and L. Mahadevan, "Shape and dynamics of tip-growing cells," Current Biology, 19, pp. 2102-2107, 2009.
- [11] O. Goriely and M. Tabor, "Self-similar tip growth in filamentary organisms," The American Physical Society, Physical Review Letters, Vol. 90, No. 10, 2003.